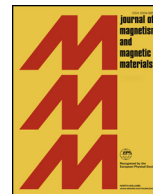




ELSEVIER

Contents lists available at ScienceDirect

## Journal of Magnetism and Magnetic Materials

journal homepage: [www.elsevier.com/locate/jmmm](http://www.elsevier.com/locate/jmmm)

## Research articles

## Investigation of size-dependent magnetic ordering in charge ordered antiferromagnetic nanoparticles via magnetocaloric effect

Kalipada Das<sup>a</sup>, Nasrin Banu<sup>b,c,\*</sup>, I. Das<sup>d</sup>, B.N. Dev<sup>b,e</sup><sup>a</sup> Department of Physics, Seth Anandram Jaipuria College, 10 Raja Naba Krishna Street, Kolkata 700005, India<sup>b</sup> Department of Materials Science, Indian Association for the Cultivation of Science, 2A and 2B Raja S. C. Mullick Road, Jadavpur, Kolkata 700032, India<sup>c</sup> Department of Condensed Matter Physics and Materials Science, Tata Institute of Fundamental Research, Homi Bhabha Road, Navy Nagar, Colaba, Mumbai 400005, India<sup>d</sup> CMP Division, Saha Institute of Nuclear Physics, 1/AF, Bidhannagar, Kolkata 700064, India<sup>e</sup> Department of Physics and School of Nano Science & Technology, Indian Institute of Technology Kharagpur, Kharagpur 721302, India

## A B S T R A C T

We have detected size-dependent modifications in magnetic ordering in charge ordered nanoparticles through the study of magnetocaloric effect. Due to prominent surface induced magnetism in nanoparticles, it is very difficult to probe the magnetic ordering in charge ordered antiferromagnetic nanoparticles from direct magnetization study, especially at lower magnetic fields, though at higher magnetic fields the antiferromagnetic/charge ordered transition can be visualized properly. We show that, at comparatively lower magnetic fields, the magnetocaloric effect provides a sensitive way for the detection of such ordering transitions.

## 1. Introduction

Surface induced predominant ferromagnetism in case of the charge ordered antiferromagnetic nanoparticles has been an intensive field of research during the past few years [1–7]. The collapse of the charge ordering or fragile nature of it has been reported by numerous researchers [1–7]. In case of the antiferromagnetic bulk materials, since bulk magnetization is very small in the presence of small external magnetic field, proper detection of different kinds of magnetic ordering is reliable only using reasonably higher fields. However, for nanoparticles of a material, the scenario is different because there is an extra magnetic contribution from the uncompensated surface spins (ferromagnetic in nature). If the particle sizes are not very small, then the both types of magnetic phases (charge ordered antiferromagnetic and ferromagnetic) co-exist. For a very small applied magnetic field the ferromagnetic component due to uncompensated surface spin is predominant whereas for higher values of the field, response from the core (antiferromagnetic) part dominates.

One can understand the nature of magnetic behavior of different kinds of magnetic compounds by studying the magnetocaloric effect [8–18]. There are some reports where the co-existence of ferromagnetic and antiferromagnetic phases was probed via the study of magnetocaloric effect [3]. However, for antiferromagnetic nanoparticles when ferromagnetic ordering is present along with charge ordering and antiferromagnetic ordering, it is very difficult to probe them by dc magnetization study. It also becomes more difficult if the two types of the

magnetic ordering are very close in the temperature scale. If the applied magnetic field is too small then the ferromagnetic signal dominates and other signals are suppressed whereas for higher magnetic fields, the opposite nature is found.

In our present study an attempt has been made to probe such different kinds of transitions precisely by using magnetocaloric effect as a powerful tool. To address such problems, we have chosen a much familiar doped perovskite manganite  $\text{La}_{0.25}\text{Ca}_{0.75}\text{MnO}_3$  compound. According to the reported phase diagram for bulk compound it exhibits charge ordering at  $T_{\text{CO}} = 270$  K and an antiferromagnetic transition at  $T_{\text{N}} = 200$  K [8]. In order to probe the size dependent magnetic behavior, we have prepared the bulk material as well as nanoparticles of average sizes of  $\sim 60$  nm (Nano-2) and  $\sim 30$  nm (Nano-1). Magnetic and magnetocaloric properties of all samples have been presented here.

For the nanoscale doped perovskite manganites with general formula  $\text{RE}_{1-x}\text{B}_x\text{MnO}_3$ , where ‘RE’ is rare earth trivalent and ‘B’ is alkaline earth bivalent elements, modification of several physical properties were reported earlier by numerous research groups [6,7,19–24]. There are many reports on non-coexistence of charge ordering or presence of fragile charge ordered state [1,2,4,6,7]. After the discovery of charge ordering in bulk compound, existence of charge ordering even in the nanocrystalline  $\text{Pr}_{0.65}\text{Ca}_{0.35}\text{MnO}_3$  compound of average particle size of  $\sim 40$  nm was reported [20]. Additionally, for even smaller particle sizes, Rao et al. reported the existence of the charge ordered fraction through the magnetic measurement at higher magnetic fields [6,7]. They also pointed out that the saturation magnetization reaches close to

\* Corresponding author.

E-mail address: [nbanu24@gmail.com](mailto:nbanu24@gmail.com) (N. Banu).<https://doi.org/10.1016/j.jmmm.2019.165309>

Received 9 April 2019; Accepted 13 May 2019

Available online 14 May 2019

0304-8853/ © 2019 Elsevier B.V. All rights reserved.

the theoretical estimated value even in nanoparticles in the presence of very high magnetic field due to the responses (melting) of the charge ordered fraction [6,7].

The aim of the present study is to address the modification of the physical properties of  $\text{La}_{0.25}\text{Ca}_{0.75}\text{MnO}_3$  compound in the nanoscale regime through the investigation of magnetocaloric effect. Along with this, our study also highlights the magnetocaloric effect as a versatile tool for the detection of several types of magnetic ordering in magnetic systems at comparatively lower magnetic fields.

## 2. Sample preparation, experimental details and characterization

Samples for the present study were prepared by the sol-gel method. For preparation of the gel, high purity (99.99%) pre-heated  $\text{La}_2\text{O}_3$  and  $\text{CaCO}_3$  were converted to their nitrate forms by using  $\text{HNO}_3$  and were dissolved into millipore water. However, to dissolve the  $\text{MnO}_2$ , suitable amount of oxalic acid was added. After completely dissolving the individual compounds, all solutions were mixed-up homogeneously in a beaker and appropriate amount of citric acid was added. After the homogeneous mixing of all individual solutions, the extra water was slowly evaporated at 80–90 °C by using a water bath until the gel was formed. The prepared gel was decomposed at slightly higher temperature (~200 °C) and black porous powder was formed. This powder was divided into three parts and pelletized individually. The pellet samples were annealed for different time spans at different temperatures to get nanoparticles of different sizes. For the preparation of different types of nanoparticles, the annealing temperature was 900 °C (for Nano-1) and 1000 °C (for Nano-2) and time duration was 4 h for each. However, for the bulk sample preparation the pelletized sample was annealed at a higher temperature (1300 °C) for a longer time period (36 hrs.).

X-ray diffraction study was carried out by Rigaku-TTRAX-III diffractometer at room temperature with  $\text{Cu-K}_\alpha$  radiation of wave length 1.54 Å. For further characterization specifically for Nano-1 and Nano-2, field emission scanning electron microscopy (FESEM) was employed. In addition to that, magnetic and magnetocaloric properties of all samples were studied by utilizing a superconducting quantum interference device-vibrating sample magnetometer (Quantum Design SQUID-VSM MPMS-III).

## 3. Results and discussions

X-ray diffraction patterns (not presented here) show the single phase nature of the all the samples. From the FESEM images the average particle sizes of the Nano-1 and Nano-2 samples were estimated. The average particle size for Nano-1 is ~30 nm and it is ~60 nm for Nano-2 sample. However, for the bulk sample the grain size is in the micrometer scale. FESEM images of bulk as well as Nano-1 and Nano-2 samples are shown in Fig. 1 for the same magnification. From the FESEM images the difference of the average particle size distribution for Nano-2 and Nano-1 is clearly evident.

### 3.1. Magnetic properties

To understand the magnetic ground state of different samples namely bulk as well as the nanomaterials (Nano-1 and Nano-2), measurement of the magnetization as a function of temperature in a low applied magnetic field of  $H = 100$  Oe has been carried out.

Magnetization measurements have been performed for all the samples in two different protocols which are zero field cooled (ZFC) and Field cooled (FC). In case of the ZFC, initially the sample was cooled down to the lowest temperature ( $T = 5$  K) from the paramagnetic state  $T = 300$  K in the absence of any external magnetic field. After stabilization of the temperature (5 K), external magnetic field  $H = 100$  Oe was applied and magnetization data were recorded during heating the sample from  $T = 5$  to 300 K (temperature increment rate was 5 K/min.). Whereas, in the FC protocol, the external magnetic field  $H = 100$

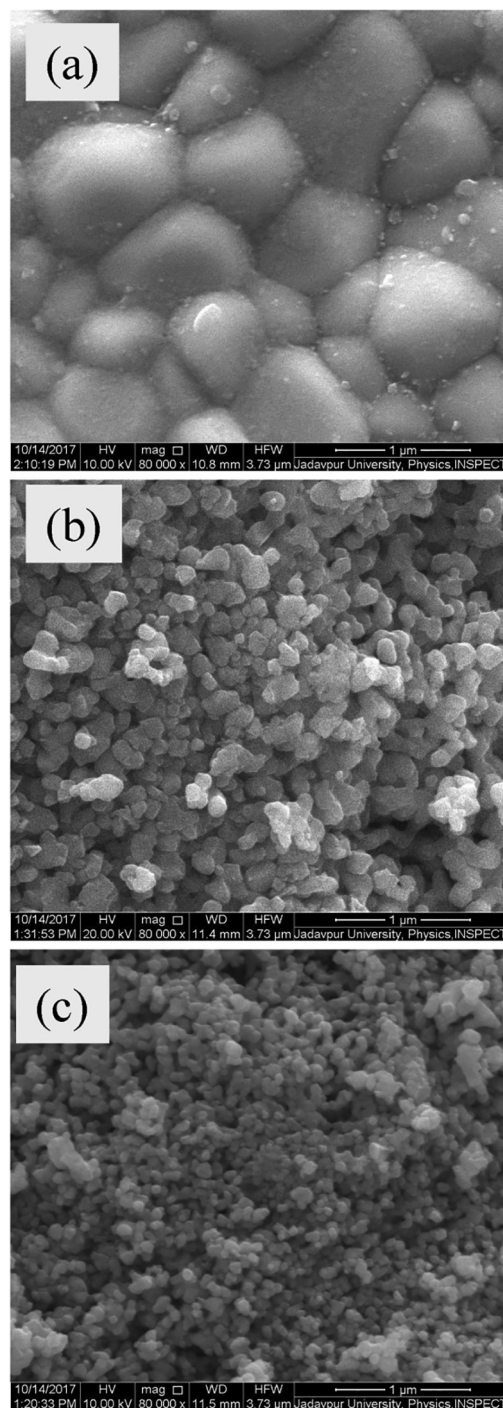


Fig. 1. Field Emission Scanning Electron Microscopy (FE-SEM) images of (a) bulk (b) Nano-2 and (c) Nano-1 samples in same magnification scale of  $\text{La}_{0.25}\text{Ca}_{0.75}\text{MnO}_3$  compound.

Oe (desired measuring field) was applied at the paramagnetic state of the sample ( $T = 300$  K in the present case) and the sample was cooled down in the presence of this magnetic field down to  $T = 5$  K. After stabilization of the temperature at  $T = 5$  K, temperature of the sample was increased at the above mentioned rate and magnetization data were recorded. Temperature dependence of the magnetization for all the samples is shown in Fig. 2(a)–(c) for bulk, Nano-1 and Nano-2 respectively. From the temperature dependent magnetization, it is clear that the bulk  $\text{La}_{0.25}\text{Ca}_{0.75}\text{MnO}_3$  compound exhibits the usual charge ordering at  $T_{\text{CO}} = 255$  K and antiferromagnetic ordering at  $T_{\text{N}} = 160$  K as reported earlier [8]. However, in the case of the nanoparticles, the

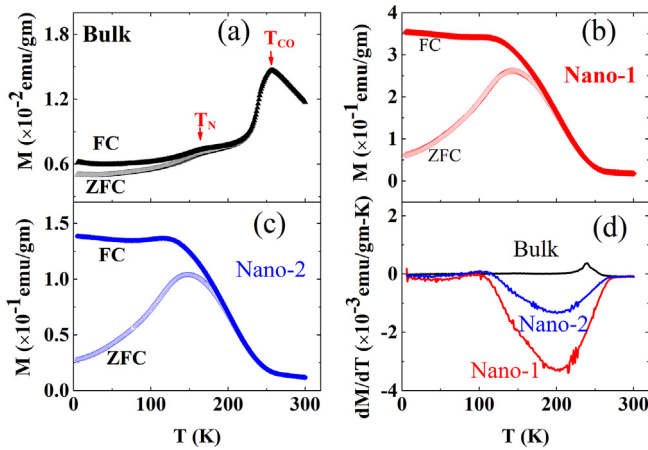


Fig. 2. (a), (b) and (c) represents temperature dependent magnetization in the presence of external magnetic field  $H = 100$  Oe of bulk, Nano-1 and Nano-2 samples respectively. (d) Derivative of field cooled magnetization (with respect to temperature) as a function of temperature for bulk, Nano-2 and Nano-1 samples.

magnetic properties are different in nature compared to their bulk counterpart. From the magnetization curves ( $M(T)$ ) for nanoparticles (Nano-1 and Nano-2), ferromagnetism dominates and neither charge ordering nor antiferromagnetic ordering was found in the presence of this low value of magnetic field. To find out the ferromagnetic ordering temperature, temperature dependence of derivatives of magnetization (with respect to temperature) is plotted in Fig. 2(d). It is worth mentioning that the temperature dependent derivative of magnetization shows a broadened ferromagnetic like transition for nano-1 and nano-2 samples. Such behaviour of magnetization in the presence of low magnetic field is associated with the orientation of the uncompensated surface spins of the nanoparticles.

The responses of the magnetization in the presence of high external magnetic fields have been studied. For the bulk material the temperature dependent magnetization at different external magnetic fields are shown in Fig. 3. For this sample, in addition to the presence of charge ordering and antiferromagnetic transition, the bifurcation between the ZFC and FC protocols almost disappears even at low temperatures. Such

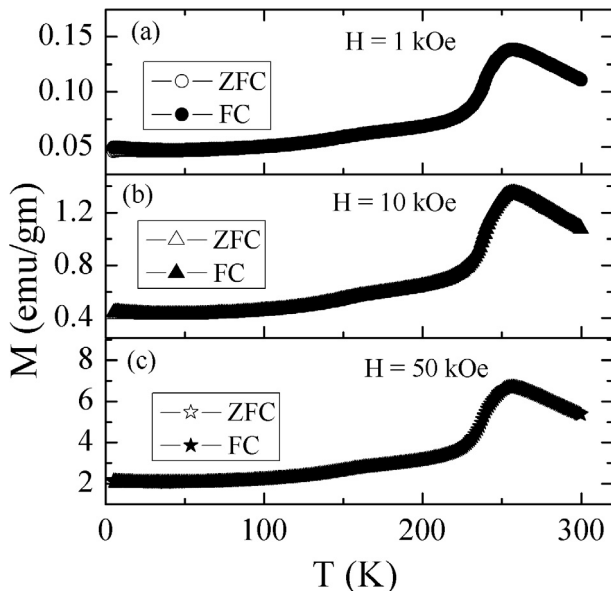


Fig. 3. Magnetization (FC and ZFC) as a function of temperature at different external magnetic field for the bulk  $\text{La}_{0.25}\text{Ca}_{0.75}\text{MnO}_3$  compound.

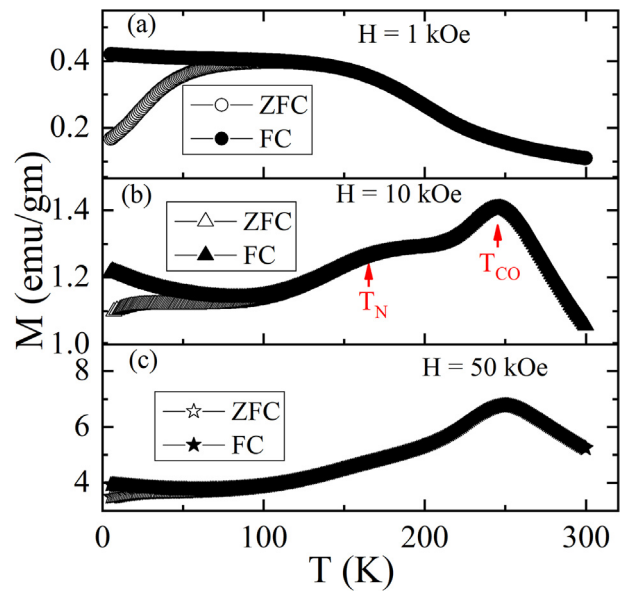


Fig. 4. Magnetization (FC and ZFC) as a function of temperature at different external magnetic field for the Nano-2 sample.

nature of the magnetization indicates the negligible anisotropy present in this bulk sample. Also the response of the magnetization for the higher values of the magnetic field qualitatively indicates the similar behaviour. However, in case of the nanoparticles the behaviour is completely different. The temperature dependence of magnetization in the presence of different external magnetic fields for nanocrystalline samples are given in Figs. 4 and 5. Our experimental results indicate that different types of the ground state appear for different values of the applied magnetic field. In the case of the nanoparticles of larger average crystalline size (nano-2), the predominant ferromagnetic like ground state is observed when the magnetization was recorded in the presence of 1 kOe external magnetic field (Fig. 4(a)). Moreover, the signatures of charge ordering and antiferromagnetic ordering are not observed. On the other hand, for sufficiently larger values of the field, namely for 10 and 50 kOe, the signatures of the above two types of transitions are clearly visible for nano-2 sample (Fig. 4(b) and (c)).

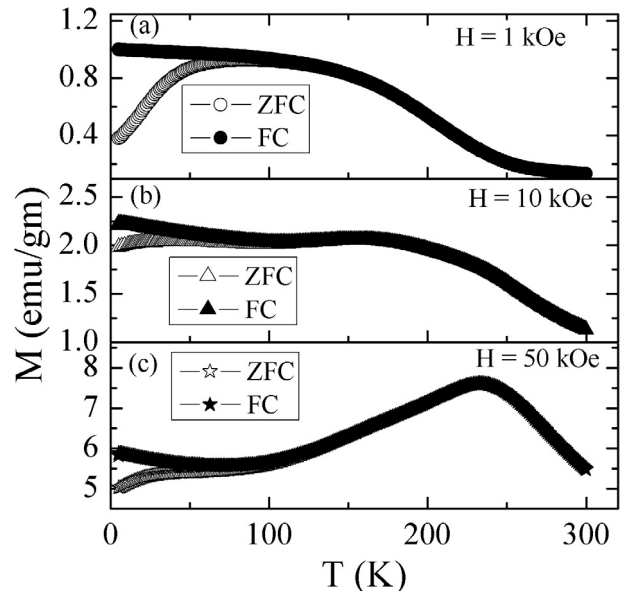


Fig. 5. Magnetization (FC and ZFC) as a function of temperature at different external magnetic field for the Nano-1 sample.

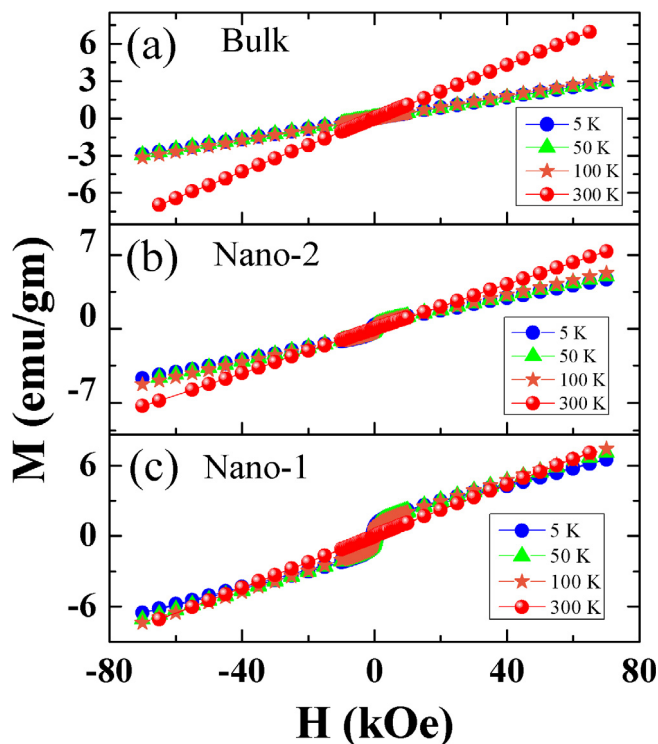


Fig. 6. External magnetic field dependent magnetization at different fixed temperature for (a) bulk (b) Nano-2 and (c) Nano-1  $\text{La}_{0.25}\text{Ca}_{0.75}\text{MnO}_3$  compound.

Contrary to Nano-2 sample, in the case of the Nano-1 sample, the antiferromagnetic and charge ordering signatures are visible only for the higher magnetic field values as shown in Fig. 5. In the presence of 1 kOe and 10 kOe external magnetic field, a ferromagnetic nature of the ground state is found.

Magnetic field dependence of the magnetization at different temperatures for the all samples are given in Fig. 6. For the bulk compound the usual antiferromagnetic nature is obtained. However, for the nanocrystalline compounds, at the lower values of the magnetic field, ferromagnetic counterpart is predominant and at higher magnetic field antiferromagnetic responses are superposed.

The magnetocaloric effect of the bulk and the nanocrystalline compounds were studied from the magnetic isotherm data by using Maxwell's thermodynamic relation which is given below

$$\Delta S = \int_0^H \left( \frac{\partial M}{\partial T} \right) dH \quad (1)$$

The calculated magnetic entropy change as a function of temperature at different external magnetic fields is given in Fig. 7. For the bulk compound, charge ordering and antiferromagnetic signatures are clearly visible in all magnetic fields (shown in Fig. 7(a)). However, for nanoparticles, the peak value of the magnetic entropy change near  $T = 270$  K gradually increases (shown in Fig. 7(b), (c)) compared to the bulk sample.

Previously, the study of the magnetocaloric effect has been widely used as an efficient tool to detect different types of feeble transitions in several systems. [25,26]. We should mention in this context that the variation of magnetocaloric entropy change ( $\Delta S$ ) with temperature is heavily modulated by the underlying magnetic ordering, even the hindered ordering, in the system under study. For example, in paramagnetic materials  $-\Delta S$  increases with decreasing temperature. For the antiferromagnetic transition (or charge ordering transition) it decreases with further reduction of temperature and change its sign (from +ve to -ve). In contrast to that, the magnetic entropy for ferromagnetic

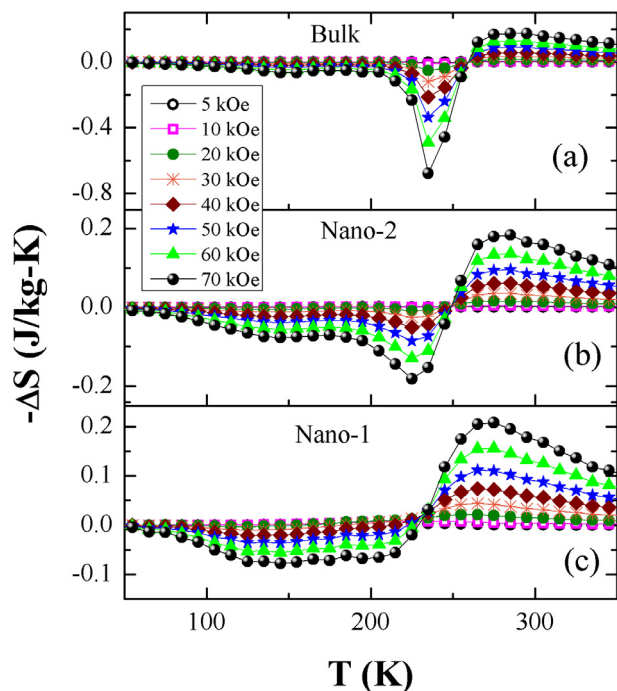
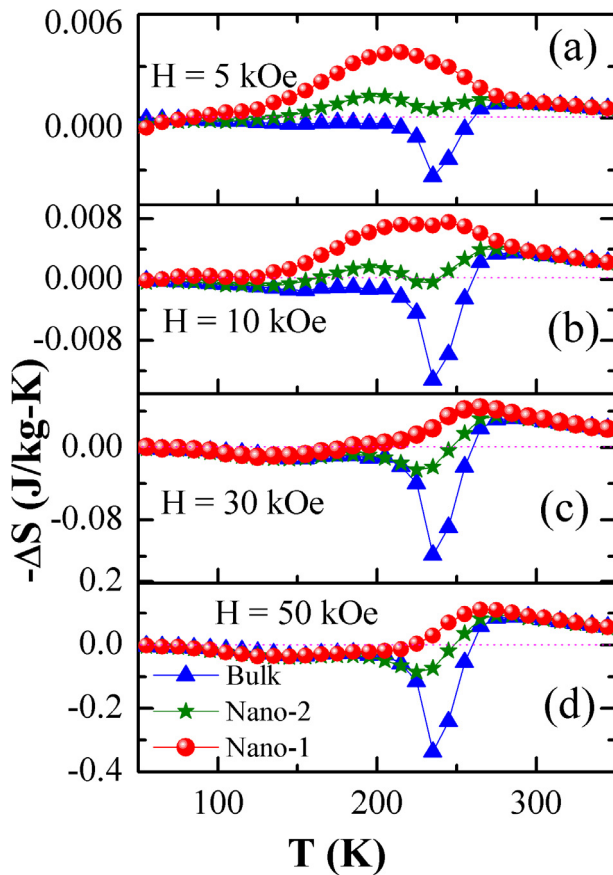


Fig. 7. Temperature dependence of isothermal magnetic entropy change at different magnetic fields for (a) bulk (b) Nano-2 and (c) Nano-1  $\text{La}_{0.25}\text{Ca}_{0.75}\text{MnO}_3$  compound.

counterpart exhibits a sharp peak (like Gaussian distribution) at the ferromagnetic transition temperature. However, in the case of phase coexistence in a sample where different types of magnetic behavior are present, the identification of ordering is quite difficult. Nevertheless, magnetocaloric study is helpful in identifying various magnetic phases. In our case, the magnetocaloric responses of the bulk and the nanoparticle systems are compared at different values of the external magnetic field (Fig. 8). We can see in Fig. 8 that for the bulk compound, charge ordering and antiferromagnetic signatures are clearly visible even at the lowest magnetic fields. But in the case of Nano-1 sample, for the external magnetic field of  $H = 5$  and 10 kOe,  $-\Delta S$  does not decrease or change sign with decrease of temperature. (A decrease or change of sign is the signature for antiferromagnetic transition or charge ordering transition). Rather it increases with decreasing temperature and reaches a peak value indicating ferromagnetic ordering within the sample. Thus, the charge ordering signature is completely suppressed in competition with the ferromagnetic counterpart for the external magnetic field of  $H = 5$  and 10 kOe. However, in the presence of higher magnetic fields (30 and 50 kOe) the signature of the antiferromagnetic ordering (charge ordering) is restored i.e.,  $-\Delta S$  decreases with decrease of temperature and finally changes its sign. The reason behind this peculiar behaviour is that for a small applied magnetic field the ferromagnetic component due to uncompensated surface spin is predominant whereas for higher values of the field, response from the core (antiferromagnetic) part dominates. Thus upon increasing the magnetic field further, similar to  $M(T)$  responses, the charge ordering nature is predominant in all studied nanocrystalline compounds.

#### 4. Summary and conclusion

To summarize our present study, we have carried out an experimental investigation for the detection of different kinds of particle size-dependent magnetic ordering in nanocrystalline  $\text{La}_{0.25}\text{Ca}_{0.75}\text{MnO}_3$  compound through the magnetocaloric effect. Additionally, the field induced modifications in magnetic ground state for nanocrystalline compounds have been probed at comparatively lower values of



**Fig. 8.** Comparison of temperature dependent magnetic entropy change at (a) 5 kOe (b) 10 kOe (c) 30 kOe and (d) 50 kOe external magnetic field.

magnetic field. Our study implies that the magnetocaloric effect can be used as a sensitive tool to elucidate the different types of modifications of the magnetic ground state of a magnetic material.

## Acknowledgement

The work was supported by Department of Atomic Energy (DAE), Govt. of India. We acknowledge the DAE-IBIQuS project (DAE OM No. 6/12/2009/BARC/R&D-I/50, Dated 01.4.2009) for the SQUID measurements.

## References

- [1] S. Dong, F. Gao, Z.Q. Wang, J.M. Liu, Z.F. Ren, *Appl. Phys. Lett.* 90 (2007) 082508.
- [2] S. Dong, R. Yu, S. Yunoki, J.-M. Liu, E. Dagotto, *Phys. Rev. B* 78 (2008) 064414.
- [3] A. Biswas, T. Samanta, S. Banerjee, I. Das, *Appl. Phys. Lett.* 92 (2008) 012502.
- [4] K. Das, P. Dasgupta, A. Poddar, I. Das, *Sci. Rep.* 6 (2016) 20351.
- [5] W.J. Lu, X. Luo, C.Y. Hao, W.H. Song, Y.P. Sun, *J. Appl. Phys.* 104 (2008) 113908.
- [6] S.S. Rao, S.V. Bhat, *J. Phys. Condens. Matter* 21 (2009) 196005.
- [7] S.S. Rao, S.V. Bhat, *J. Phys. Condens. Matter* 22 (2010) 116004.
- [8] S.W. Cheong, H.Y. Hwang, *Contribution to Colossal Magnetoresistance Oxides, Monographs in Condensed Matter Science*, Gordon and Breach, London, 1999.
- [9] H. Wada, Y. Tanabe, *Appl. Phys. Lett.* 79 (2001) 3302–3304.
- [10] H. Wada, Y. Tanabe, M. Shiga, H. Sugawara, H. Sato, *J. Alloys Compd.* 316 (2001) 245–249.
- [11] T. Tohei, H. Wada, *J. Magn. Magn. Mater.* 280 (2004) 101–107.
- [12] N.K. Singh, K.G. Suresh, A.K. Nigam, S.K. Malik, *J. Appl. Phys.* 97 (2005) 10A301.
- [13] M.H. Phan, S.C. Yu, *J. Magn. Magn. Mater.* 308 (2007) 325.
- [14] A.M. Tishin, Y.I. Spichkin, *The Magnetocaloric Effect and its Applications*, Institute of Physics Publishing, Bristol and Philadelphia, 2003.
- [15] K.A. Gschneidner Jr., V.K. Pecharsky, A.O. Tsokol, *Rep. Prog. Phys.* 68 (2005) 1479–1539.
- [16] N.A. de Oliveira, P.J. von Ranke, *Phys. Rep.* 489 (2010) 89–159.
- [17] A.O. Pecharsky, K.A. Gschneidner Jr., V.K. Pecharsky, *J. Appl. Phys.* 93 (2003) 4722–4728.
- [18] O. Tegus, E. Bruck, K.H.J. Buschow, F.R. deBoer, *Nature (London)* 415 (2002) 150–152.
- [19] A. Biswas, I. Das, *Phys. Rev. B* 74 (2006) 172405.
- [20] K. Das, B. Satpati, I. Das, *RSC Adv.* 5 (2015) 27338.
- [21] K. Das, R. Rawat, B. Satpati, I. Das, *Appl. Phys. Lett.* 103 (2013) 202406.
- [22] A. Biswas, I. Das, *J. Appl. Phys.* 102 (2007) 064303.
- [23] A. Biswas, I. Das, C. Majumdar, *J. Appl. Phys.* 98 (2005) 124310.
- [24] M.H. Phan, S. Chandra, N.S. Bingham, H. Srikanth, C.L. Zhang, S.W. Cheong, T.D. Hoang, H.D. Chinh, *Appl. Phys. Lett.* 97 (2010).
- [25] Tapas Samanta, I. Das, S. Banerjee, *J. Appl. Phys.* 104 (2008) 123901.
- [26] Tapas Paramanik, Kalipada Das, Tapas Samanta, I. Das, *J. Magn. Magn. Mater.* 381 (2015) 168.